ELSEVIER

Journal of Alloys and Compounds 323–324 (2001) 847–850

Journal of ALLOYS AND COMPOUNDS

www.elsevier.com/locate/jallcom

Solar ultraviolet-B detectors using Eu^{2+} doped alkali halide crystals

C. Cordoba-Jabonero[a,*], I. Aguirre de Carcer[b], M. Barboza-Flores[c], F. Jaque[b]

[a]*Centro de Astrobiología, C.A.B. (CSIC-INTA), Madrid, Spain*
[b]*Departamento de Física de Materiales, Universidad Autónoma de Madrid, Madrid, Spain*
[c]*Centro de Investigaciones en Física, Universidad de Sonora, Hermosillo, Mexico*

Abstract

The continuous depletion of the ozone layer causes an increase in the ultraviolet-B (UV-B) reaching the Earth's surface. In this paper the behaviour of the KCl:Eu^{2+} under solar UV irradiation has been investigated. Considering the thermoluminescence (TL) excitation spectra, the geometrical solar radiation parameters (solar zenith angle related to the light path) and the atmosphere characteristics (ozone content, Rayleigh scattering and aerosols' concentration), the solar UV irradiation flux registered by the dosimeter has been simulated throughout the day. This modelled hourly signal agrees with the measured TL signal at different hours. Moreover, these curves throughout the day are compared to the convoluted signal obtained from a gaussian curve centred at different UV-C wavelengths and the same solar spectrum. This comparison supports the idea that the KCl:Eu^{2+} crystal behaves under the sun as a narrow band gaussian detector centred at about 265 nm, but with the main registered solar UV-B signal at 285 nm. On the other hand, a comparison of the KCl:Eu^{2+} system with commercially available broad band UV-B biological sensors (biometers), shows that the europium doped crystals are more sensitive to minor changes of the solar UV-B flux and therefore, it is a good instrument for the study of small ozone layer depletions. © 2001 Elsevier Science B.V. All rights reserved.

Keywords: Thermoluminescence dosimetry; Solar UV radiation; Eu^{2+} doped alkali halide crystals; UV biosensors; Environmental applications

1. Introduction

Solar ultraviolet B (UV-B, 280–320 nm) radiation in the northern hemisphere is increasing due to the systematic ozone depletion in that region [1]. The depleted ozone filter is allowing increasing amounts of high-energy photons to reach the troposphere and is thus affecting the functioning of the biosphere. The necessity for estimating UV-B flux interacting with the biosphere is an important environmental issue because its magnitude and its variability within different habitats will change, yet in an unknown way, the distribution of species [2–4]. Furthermore, since the high energy UV photons cause higher damage to biological specimens than lower energy UV-B photons, the determination of the solar UV high energy fluxes reaching the Earth's surface is of great importance for the simulation of the biological effects of the depletion of the ozone layer.

The solar UV radiation reaching the Earth's surface has a strong variation of intensity between 250 and 410 nm; there is approximately 30 times stronger irradiance at the lower energy side than at the high energy side of that band [5]. However, high energy solar UV-B is difficult to measure using scanning spectroradiometers which under solar irradiation fail at wavelengths below 290 nm, for which a very high stray-light suppression factor of 10^{-8} is needed [6]. The development of new materials has shown the possibility of determining solar ultraviolet radiation dose using f-elements impurities in several matrixes [7–10].

It has been proven that high-energy UV-B photons cause damage on alkali halide crystals doped with Eu^{2+} linearly proportional to the incident irradiation flux. In this material, the $^8S_{7/2}(4f^7) \rightarrow E_g(4f^6 5d)$ Eu^{2+} optical transition in the UV range triggers a mechanism which at its first step produces an electron trapped in the matrix near to a divalent europium impurity. The trapped electron is thermally released from the trap and recombines with the perturbed europium impurity, emitting finally a thermoluminescence (TL) blue emission [11–13] restoring the crystal to its initial condition. Fortunately, the first TL glow peak is found at temperatures around 90°C, so an appropriate selection of irradiation damage temperature, storing temperature and filtering photobleaching wavelengths allow us to measure solar short wavelength UV-B dose. Thus, the UV-B irradiation can be ascertained using

*Corresponding author.

0925-8388/01/$ – see front matter © 2001 Elsevier Science B.V. All rights reserved.
PII: S0925-8388(01)01158-6

themoluminescence (TL) or optically stimulated luminescence (OSL) without the aforementioned stray light problem as the crystal is effectively insensitive to longer wavelengths. Those systems are very sensitive to UV-B and the TL signal is obtained after few seconds of solar exposure.

Solar UV irradiance at the Earth's surface and the TL excitation spectrum of the KCl:Eu^{2+} single crystals have a small overlap, so the effective solar UV range activating the crystals is a relevant question. Preliminary results using a newtonian telescope with a large collecting area and a high intensity monochromator (blaze 300 nm, 2 nm wavelength bandpass) directed to the sun with a UV-pass filter interposed showed that the outdoor excitation spectrum consisted of a narrow band centred at 260 nm [14]. On that occasion the experimental excitation spectrum obtained could be modelled as the convolution of the KCl:Eu^{2+} laboratory excitation spectrum with a simulated solar spectrum at ground level calculated by a radiative transfer model. In this work the KCL:Eu^{2+} TL solar activation has been confirmed using an indirect method, measuring the relative solar UV reaching the ground at a particular location, at different hours.

1.1. Experimental and results

The solar UV-B flux at the Earth's surface varies, mainly with the following factors: atmospheric total ozone content, presence of scattering aerosols, cloud cover and solar zenith angle (related to the air mass that light must transverse before reaching the surface). Therefore, the solar short wavelength UV-B irradiance reaching the surface can be simulated using a 'two-stream' radiative transfer model mainly accounting for at least the ozone content and the solar zenith angle, and to a lesser extent for the aerosols concentration and cloud cover [15]. The results of simulation can be compared with experimental data obtained from measurements taken at different hours of the day.

The KCl:Eu^{2+} (150 ppm) dosimeter was exposed for 2 min to the solar radiation, at ambient temperature, several times throughout the day, using an ultraviolet pass filter (spectral response shown in Fig. 1, inset) in order to avoid photobleaching of the TL signal. Glow curves were obtained using a hot nitrogen gas TL reader, Panasonic UD513A, with a 30°C s^{-1} heating rate. Fig. 1 shows the experimental TL signal versus solar time registered at Cantoblanco (Madrid, 40° N, 3° W, 700 m a.s.l.) on a clear sky day (04/24/1998) with a total ozone content of 326 Dobson Units (D.U.). From Fig. 1 it can be seen that the registered UV TL signal only departs from zero around solar midday (minimum solar zenith angle), resulting in a skew curve (line to 'guide the eye' at Fig. 1) throughout the day. This is the expected behaviour of the TL dosimeter signal at the ozone absorption wavelengths. For this reason it can be ascertained that the KCl:Eu^{2+} dosimeter is effectively blind for solar wavelengths in the UV-A band, where the solar irradiance is very high due to the negligent ozone absorption in this band. In Fig. 1 it is also shown the experimental signal (normalised) registered along the day by Solar Light 501A (SL 501A) for the same day (04/24/1998). This curve is much broader than the one for the TL dosimeter, showing the SL 501A instrument by contrast registers solar UV radiation mainly in a broad UV-B band close to the UV-A band. The TL experimental data in Fig. 1 show some structure around noon that could be interpreted as a decrease in solar UV radiation resulting from transient tropospheric ozone transport over the dosimeter site.

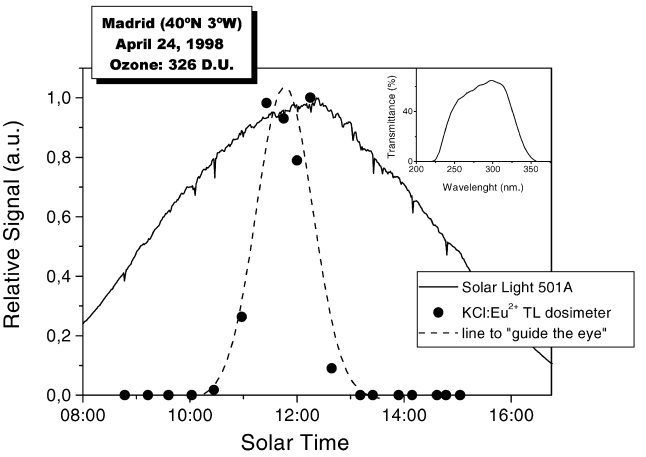

Fig. 1. Experimental data: KCl:Eu^{2+} TL dosimeter and SL 501A signals under exposure to environmental solar UV radiation.

From Fig. 1 it is possible to examine which is the particular range of solar wavelengths that give rise to the TL signal and to attempt to answer the question of which wavelength band is the dosimeter really measuring under solar exposure. For that purpose, first, the KCl:Eu^{2+} TL solar excitation has been assimilated to a gaussian function (the laboratory TL excitation function resembles a gaussian fuction and its convolution with solar irradiance in a small band of the UV-C, UV-B range should not alter significantly that shape), whose centre band (λ_0) and full width at half maximum (FWHM) are used as parameters to be obtained by data fitting. The next step consists of convoluting the spectral distribution of the solar UV-B irradiance provided by the simulation with the 'two-stream' radiative transfer model at several hours throughout the day with different possible TL equivalent dosimeters (TL–ED) responses (different gaussian functions resulting from different values of parameters λ_0 and FWHM) [16]. Fig. 2 shows the experimental data (dots) and the convolution curves (dashed lines) obtained for three different values of parameter λ_0 in the UV-C band: 260, 270 and 280 nm, for the TL-ED throughout the day. In all cases, a fixed FWHM value of 5 nm was considered because of the small overlap between the laboratory TL excitation range and the wavelengths for which solar irradiances are significant.

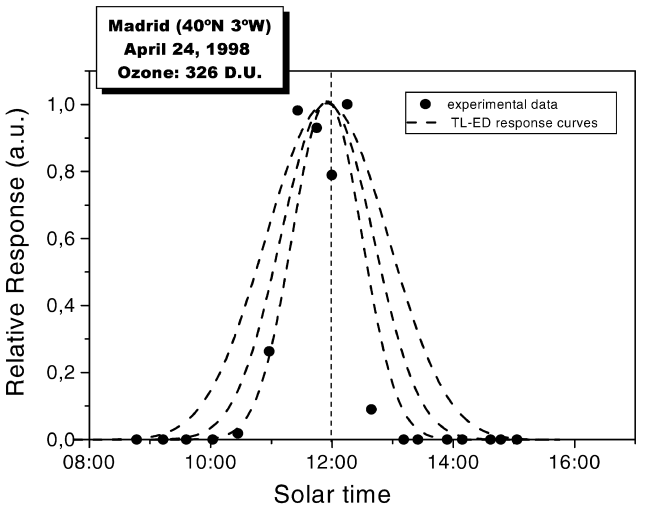

Fig. 2. Experimental data and gaussian curves of TL–ED for λ_0=260, 270 and 280 nm (from inside to outside, respectively).

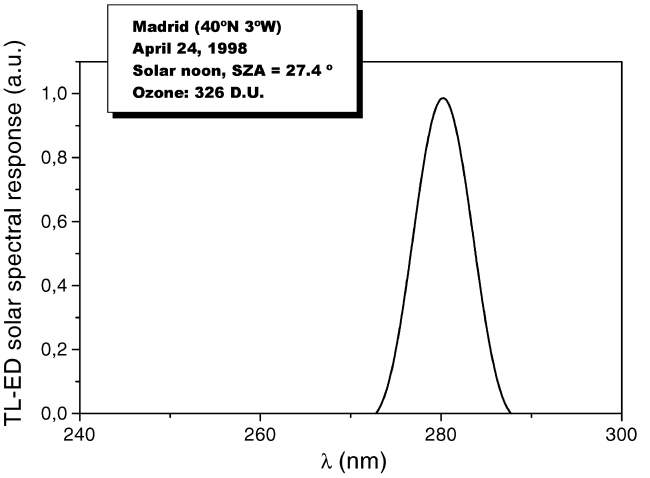

Fig. 3. Convolution of TL–ED gaussian function with parameter λ_0=265 nm (FWHM=5 nm) and the solar spectrum reaching the surface.

As it can be observed, the best fitting is obtained for a value of parameter λ_0=265 nm (being FWHM=5 nm). The erythema biological UV radiation, as measured by SL 501A, can be fitted to a equivalent gaussian function too, obtaining a best fitting for values of parameters λ_0=305–310 nm and FWHM=10 nm. This result confirms what was found earlier with the experimental data: the KCl:Eu^{2+} TL dosimeter could register radiation in the UV-C close to UV-B solar band, and the SL-501A in the UV-B close to UV-A band.

On the other hand, the solar irradiation reaching the surface is very weak at 265 nm and increases abruptly at longer wavelengths. Inside the UV-C band, the solar spectrum is much more intense at wavelengths close to the UV-B band so a response shift to higher wavelengths takes place, phenomenon known as Forbes effect [17]. At midday (minimum solar zenith angle), the convolution of the response curve of the TL–ED and the solar spectral irradiance distribution gives a maximum for λ_0=280–285 nm, corresponding to the UV-B band, very close to the UV-C band (Fig. 3). By contrast, the SL 501A effective wavelength response varies only slightly with the solar zenith angle due to its broad band in the UV-B range. As a consequence, the KCl:Eu^{2+} TL dosimeter signal varies a great deal with minor changes of the total ozone content while only minor changes are observed in the SL 501A signal.

Fig. 4 shows the experimental data obtained with SL 501A and the TL dosimeter taken in Madrid on the 05/18/1998 with total ozone content of 341 D.U. where changes in the UV-B atmospheric transmission (arrows) are evidenced, probably due to tropospheric ozone transport over the measuring site. It can be appreciated in Fig. 4 that the hypothesised changes in the atmosphere produce important variations in the UV-B radiation registered by the KCl:Eu^{2+} TL dosimeter (high energy photons) while the corresponding changes in the SL 501A signal are less pronounced because it also measures irradiance at wavelengths where ozone absorption is rather small.

2. Conclusions

The reported data and analysis support the idea that the KCl:Eu^{2+} crystal TL dosemeter behaves under the solar radiation as a narrow band gaussian shaped detector centred at about 265 nm which registers mainly solar UV-B flux at 280–285 nm. The KCl:Eu^{2+} dosimeter compares favourably with commercially available broad band UV-B biological sensors (biometers) because it does not register UV-A or low energy UV-B photons and does not need filters, which always mitigate the impinging irradiance. The experimental data obtained so far shows

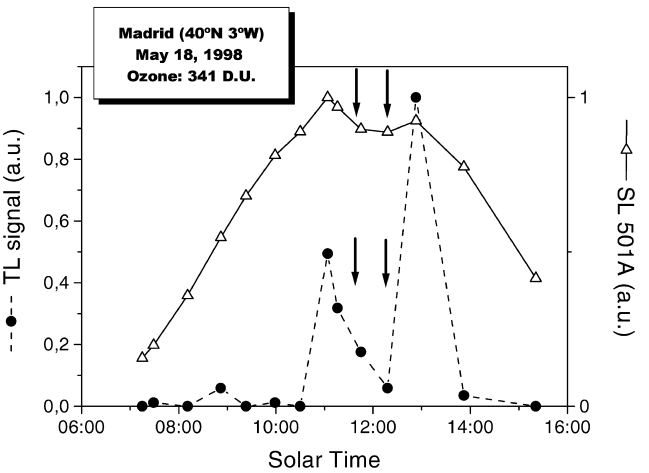

Fig. 4. Experimental data: different variation of the signal registering solar UV radiation mainly in the UV-C close to UV-B band by KCl:Eu^{2+} TL dosimeter (full circles) and in the UV-B close to UV-A band by SL 501A (open triangles) under changes in the atmospheric UV transmission (arrows).

that the KCl:Eu^{2+} dosimeter is more sensitive to minor changes of the solar UV flux than biometers and therefore, it could be the core of good instruments for the study of small ozone layer depletions. The analysis of solar UV irradiance reaching the Earth's surface with other f-elements systems may help the scientific community to realise the existence of high energy UV photons interacting with the biota (current action spectra are evaluated only for wavelengths above 290 nm while in some cases the maximum biological damage is obtained at lower wavelengths).

References

[1] R. Bojkov et al., J. Geophys. Res. 102 (D1) (1997) 1337.
[2] M. Tevini, UV-B Radiation and Ozone Depletion: Effects On Humans, Animals, Plants, Micro-organisms and Materials, Lewis Publishers, Boca Raton, FL, 1993.
[3] R. Smith et al., Science 255 (1992) 952.
[4] W. Friedrich, in: W.F. Passchier, B.F.M. Bosnjakovic (Eds.), Risk-benefit Evaluation of UV-exposure, Human Exposure To Ultraviolet Radiation Risks and Regulations, Elsevier, Amsterdam, 1987.
[5] L. Molina, M. Molina, J. Geophys. Res., D 19 (1986) 14501.
[6] H. Tüg, M.E. Baumann, Geophys. Res. Lett 21 (1994) 689.
[7] M. Barboza-Flores et al., Radiat. Meas. 29 (5) (1998) 487.
[8] H. Nanto et al., Radiat. Protect. Dosim. 85 (1–4) (1999) 305.
[9] S. Nakamura et al., Radiat. Protect. Dosim. 85 (1–4) (1999) 313.
[10] J. Azorin et al., Radiat. Protect. Dosim. 85 (1–4) (1999) 317.
[11] F. Jaque et al., Health Phys. 60 (1991) 579.
[12] I. Aguirre de Carcer et al., Appl. Phys. Lett. 58 (1991) 1825.
[13] I. Aguirre de Carcer et al., Radiat. Meas. 29 (2) (1998) 203.
[14] C. Cordoba et al., J. Phys. D: Appl. Phys. 30 (1997) 3024.
[15] M. Iqbal, An Introduction to Solar Radiation, Academic Press, Toronto, 1983.
[16] C. Cordoba et al., Radiat. Protect. Dosim. 85 (1–4) (1999) 321.
[17] R.E. Basher, J. Appl. Meteorol. 16 (1977) 803.